1962

Investigation of a divergent barotropic prediction model for the 300-MB level.

Oakes, Winslow B.

Monterey, California. Naval Postgraduate School

INVESTIGATION OF A DIVERGENT BAROTROPIC PREDICTION MODEL FOR THE 300-MB LEVEL

WINSLOW B. OAKES

52

INVESTIGATION OF A DIVERGENT BAROTROPIC PREDICTION MODEL FOR THE 300-MB LEVEL

* * * * *

Winslow B. Oakes

INVESTIGATION
OF A
DIVERGENT BAROTROPIC
PREDICTION MODEL
FOR THE
300-MB LEVEL

by

Winslow B. Oakes
Lieutenant, United States Navy

Submitted in partial fulfillment of
the requirements for the degree of

MASTER OF SCIENCE
IN
METEOROLOGY

United States Naval Postgraduate School
Monterey, California

1962

INVESTIGATION OF A DIVERGENT BAROTROPIC PREDICTION MODEL FOR THE 300-MB LEVEL

by

Winslow B. Oakes

This work is accepted as fulfilling
the thesis requirements for the degree of
MASTER OF SCIENCE
IN
METEOROLOGY
from the
United States Naval Postgraduate School

ABSTRACT

The usefulness of a barotropic prediction model for providing realistic displacements at levels other than 500 mb is suggested to circumvent difficulties with current baroclinic models attempting to predict development as well.

A prediction equation is obtained by making use of concepts from Charney's equivalent barotropic model, 'Arnason's stratified model, and Cressman's semi-empirical barotropic model. Further, a stream-function prediction scheme, making use of geostrophic and non-divergent wind relationships, is used to make a series of 24- and 48-hour forecasts of 300-mb heights. The vorticity equation used is

$$\left(\nabla^2 - K_1 \frac{\mu f_m \eta}{g \bar{z}_{500}}\right) \frac{\partial \psi}{\partial t} + J(\psi, K_2 \zeta + f) - K_3 \frac{\mu f_m \eta}{g \bar{z}_{500}} J(\bar{\psi}, \psi) = 0$$

where K_1, K_2, and K_3 are empirical constants. Results are presented for the effects of adjusting K_2 and K_3.

The author wishes to express his appreciation to Professor George J. Haltiner of the U. S. Naval Postgraduate School for his guidance and encouragement in this investigation.

Appreciation is also expressed to the personnel of the U. S. Fleet Numerical Weather Facility for their assistance in this project. Special thanks are extended to Lieutenants Mildred J. Frawley and Harry E. Nicholson and Mr. Milton H. Reese for assistance in programming and many helpful suggestions.

TABLE OF CONTENTS

LIST OF ILLUSTRATIONS

TABLE OF SYMBOLS

ζ - The relative vorticity. $\zeta = k \cdot \nabla \times V$.

η - The absolute vorticity. $\eta = \zeta + f$.

f - The Coriolis parameter, $2\Omega \sin \varphi$, where φ is the geographic latitude.

f_m - The mean value of the Coriolis parameter, $2\Omega \sin 45$.

ω - The vertical wind component in the x, y, p, t coordinate system. $\omega = \frac{\partial p}{\partial t}$.

g - The upward component of the apparent gravitational acceleration.

Φ - The geopotential. $\Phi = gz$.

ψ - The stream function for the non-divergent component of velocity.

∇^2 - The horizontal Laplacian operator on a constant pressure surface.

∇_n^2 - The finite-difference equivalent of ∇^2.

$J(A,B)$ - The horizontal Jacobian operator. $J(A,B) = \frac{\partial A}{\partial x}\frac{\partial B}{\partial y} - \frac{\partial A}{\partial y}\frac{\partial B}{\partial x}$.

$J(A,B)$ - The finite-difference equivalent of $J(A,B)$.

$\frac{\Delta A}{\Delta B}$ - The finite-difference equivalent of the derivative, $\frac{\partial A}{\partial B}$.

1. Introduction.

Up to the present time, most attempts to predict the pressure height at levels other than 500 mb have been made with baroclinic models. The results have been disappointing because of inadequately controlled development mechanisms. Observing the persistent skill of barotropic forecasts at 500 mb, 'Arnason [1] suggested the possiblity of devising a barotropic prediction model to be applied to other levels, "capable of realistic displacements of pressure systems...but containing no mechanism for development."

This investigation introduces an empirically adjusted divergent barotropic model for application to the 300-mb surface. Concepts from Charney's [2] equivalent barotropic model and 'Arnason's stratified model [1] are incorporated in addition to empirical results by Cressman [3] on control of very long atmospheric waves.

2. Background.

Looking first to the equivalent barotropic model, it is recalled that partial baroclinicity is permitted in that wind speed, but not direction, is allowed to vary with height at any point. If the integrated mean of this wind with respect to pressure is determined, the wind, $\mathbb{V}$, and vorticity, ζ, at any level can be expressed as a scalar factor, A, of this mean. For further simplicity, A is considered to be a function of pressure alone. Thus

$$\mathbb{V} = A(p)\,\hat{\mathbb{V}}, \qquad \zeta = A(p)\,\hat{\zeta}, \tag{2.1}$$

where the cap indicates the vertically integrated mean. Climatologically, $\hat{\mathbb{V}}$ is observed to occur at about 600 mb.

Substituting the expressions (2.1) in the approximate vorticity equation

$$\frac{\partial \zeta}{\partial t} + \mathbb{V}\cdot\nabla(\zeta + f) = f_m \frac{\partial \omega}{\partial p}$$

and integrating with respect to pressure gives

$$\frac{\partial \hat{\zeta}}{\partial t} + \hat{\mathbb{V}}\cdot\nabla(\hat{A}^2\hat{\zeta} + f) = 0. \tag{2.2}$$

Here f is the coriolis parameter, and $\hat{A}^2$ is found empirically to have a value of about 1.25. Multiplying (2.2) by $\hat{A}^2$ and substituting $\hat{A}^2\hat{\zeta} = \zeta^*$ and $\hat{A}^2\hat{\mathbb{V}} = \mathbb{V}^*$ forms the basis for barotropic forecasts at the <u>equivalent barotropic level</u>, (p^*), occurring in nature at about 500 mb.

If, however, the expressions (2.1) are substituted for $\hat{\mathbb{V}}$ and $\hat{\zeta}$ into (2.2), the following is obtained:

$$\frac{\partial \zeta}{\partial t} + \mathbb{V}\cdot\nabla(K_2\zeta + f) = 0, \tag{2.3}$$

where $K_2 = \frac{\hat{A}^2}{A}$. For the wind field (2.1), equation (2.3) applies to any level with the K_2 appropriate to that level.

In applying the theory of the stratified model to forecasting, 'Arnason arrives at an expression for divergence

$$\nabla \cdot \mathbb{V} = -\frac{1}{g'H}\left(\frac{\partial \bar{\Phi}}{\partial t} + \bar{\mathbb{V}} \cdot \nabla \bar{\Phi}\right) , \tag{2.4}$$

where $\bar{\Phi}$ is geopotential, $\bar{\mathbb{V}}$ is the basic flow, and H is the thickness of the stratified layer. The parameter, g', is related to gravity, although much smaller, and depends upon static stability and the vertical extent of the stratified layer. This expression for divergence is introduced into the vorticity equation

$$\frac{\partial \zeta}{\partial t} + \mathbb{V} \cdot \nabla \eta_2 + \eta \nabla \cdot \mathbb{V} = 0 \tag{2.5}$$

to give

$$\frac{\partial \zeta}{\partial t} + \mathbb{V} \cdot \nabla \eta_2 - \frac{\eta}{g'H}\left(\frac{\partial \bar{\Phi}}{\partial t} + \bar{\mathbb{V}} \cdot \nabla \bar{\Phi}\right) = 0 , \tag{2.6}$$

where $\eta = \zeta + f$ is absolute vorticity; η_2 is defined for our purposes as $\eta = K_2 \zeta + f$ of (2.3).

The prediction scheme consists of introducing a stream function, ψ, to represent the wind and vorticity

$$\mathbb{V} = \mathbb{k} \times \nabla \psi , \quad \zeta = \nabla^2 \psi \tag{2.7}$$

where $\mathbb{k}$ is the unit vector in the vertical. The stream function is initially obtained from the balance equation

$$f\nabla^2 \psi + 2\left(\psi_{xx}\psi_{yy} - \psi_{xy}^2\right) + \nabla \psi \cdot \nabla f - \nabla^2 \bar{\Phi} = 0 . \tag{2.8}$$

Next, in order to simplify the procedure, the quasi-geostrophic relation-

ship

$$\Phi = f\psi \tag{2.9}$$

is introduced into the divergence term. The result of substituting (2.7) and (2.9) into (2.6) is

$$\frac{\partial}{\partial t}\nabla^2\psi + J(\psi, \eta_2) - \frac{f\eta}{g'H}\left[\frac{\partial \psi}{\partial t} + J(\bar{\psi}, \psi)\right] = 0$$

or

$$\left(\nabla^2 - \frac{f\eta}{g'H}\right)\frac{\partial \psi}{\partial t} + J(\psi, \eta_2) - \frac{f\eta}{g'H} J(\bar{\psi}, \psi) = 0\,, \tag{2.10}$$

where $\bar{\psi}$ is the stream function corresponding to the basic flow. Equation (2.10) is a prognostic equation in a single variable, ψ.

3. Procedure.

Application of 'Arnason's stratified model involves an interpretation of the parameters, $\overline{\psi}$, g', and H. Also, the introduction of a factor, K_1, into the tendency portion of the divergence term, and a factor, K_3, into the advection portion of the divergence term permits adjustment of the magnitude of these terms for various levels.

The basic flow for this prediction model is taken as a spaced-averaged flow at 300 mb, employing a 15-pass, 4-point smoother over the finite-difference grid used for computations (grid distance equal to 381 km at 60N latitude):

$$\overline{\psi}_0 = \frac{1}{4}\left(\psi_1 + \psi_2 + \psi_3 + \psi_4\right) \tag{3.1}$$

The subscript zero denotes the central point of a diamond array and the subscripts one through four denote the surrounding four grid points.

In arriving at an interpretation of g', reference is made to Cressman's [3] treatment of a model including a dependence upon static stability. He introduced a stability parameter, μ, which as applied here amounts to a substitution of

$$\frac{\mu}{g} = \frac{1}{g'} \tag{3.2}$$

In a series of 500-mb forecasts Cressman used various values of μ in his divergent barotropic model. It was concluded that $\mu = 4$ affords the desired control on the ultra-long waves, and gives better forecasts than a former Joint Numerical Weather Prediction Unit forecast model. Use has been made of this value by the substitution of (3.2) into (2.10).

In addition, the mean value $\frac{g\bar{Z}_{500}}{f_m}$ has been used for $\frac{gH}{f}$ (similar to Cressman), taking $\bar{Z}_{500}$ as the U. S. standard atmosphere 500-mb height,

and $f_m = f$ at 45N latitude.

With these last adjustments, (2.10) becomes

$$\left(\nabla^2 - K_1 \frac{\mu f_m \eta}{g \bar{z}_{500}}\right) \frac{\partial \psi}{\partial t} + J(\psi, K_2 \zeta + f) - K_3 \frac{\mu f_m \eta}{g \bar{z}_{500}} J(\bar{\psi}, \psi) = 0 . \qquad (3.3)$$

In finite difference form, (3.3) becomes

$$\left(\nabla^2 - K_1 \frac{\mu f_m \eta}{g \bar{z}_{500}} \frac{d^2}{K_1 a}\right) \frac{\Delta \psi}{\Delta t} + \frac{1}{4} \mathcal{J}(\psi, K_2 \zeta + f) - K_3 \frac{\mu f_m \eta}{4 g \bar{z}_{500}} \mathcal{J}(\bar{\psi}, \psi) = 0 , \qquad (3.4)$$

where ∇^2, Δ, and $\mathcal{J}$ are the finite-difference equivalents of the Laplacian, differential, and Jacobian operators, respectively; and $\frac{d}{m}$ is the sea-level distance between grid points. Forecasts are made in one-hour time steps, using a forward difference for the first step and centered differences for successive steps.

Equation (3.4) was programmed for the Control Data Corporation Model 1604 computer using U. S. Fleet Numerical Weather Facility's 1977-point octagonal grid, which covers the Northern Hemisphere from pole to about 10N.

Step one in the forecasting procedure consists of solving the balance equation for an initial stream function, using analyzed D-values (deviation in height from standard). A technique formulated and programmed for the CDC 1604 by 'Arnason and Reese at the Fleet Numerical Weather Facility was used. It was found that for most of the 300-mb data available for this investigation, this method would not converge to the cut-off criterion (all residuals less than 0.5 feet in the relaxation procedure as normally used at lower levels). In order to proceed with the work, an arbitrary cut-off was introduced if non-convergence became apparent. This introduced errors at a few points of the grid due to residuals which were now of the order of three to five feet. These were considered to be insignif-

icant with respect to the prediction scheme.

Step two was solution of equation (3.4), and this was repeated on each day's data using various values of the factors K_2 and K_3. The factor K_1 was taken equal to one and not adjusted in this investigation. Values of K_2 and K_3 were chosen as work progressed so as to reduce forecast errors to a minimum.

Step three consisted of verifying the forecasts against the prepared analyses by a simple point-by-point difference, and calculation of the pillow and root-mean-square error (RMSE):

$$\text{Pillow} = \frac{1}{x}\sum_{n=1}^{x}(A-B)_n \;, \quad \text{RMSE} = \left[\frac{1}{x}\sum_{n=1}^{x}(A-B-\text{Pillow})_n^2\right]^{1/2} \tag{3.5}$$

x = 1977 points, A = forecast map, B = analysis map.

4. Results.

Table 4.1 lists the results of adjusting the factor K_3 with K_2 held equal to one. Numbers to the left of each column are pillow while the numbers to the right are RMSE. Upper numbers of each paired set are for 24-hour forecasts and lower numbers are for 48-hour forecasts.

Runs were not made for all included values of K_3 but minimum errors were sought. The numbers in parentheses are values taken from faired curves through the values that were run. Fig. 4.1 shows the curves for 24-hour forecasts; those for 48-hour forecasts would be similar. The trends of errors for the successive values of K_3 were observed to be quite regular, thus justifying an approximation of intermediate values where necessary for the averages over all days. In cases where actual reversal of error trends was not observed, the fact that differences between successive values of K_3 were reduced to zero or one foot was taken as an indication that reversal was imminent, and adjustments of K_3 were terminated.

In one case (17 January) a forecast was made using a positive value of K_3, showing an error much larger than the optimum for this day. Other work on this term not presented here further confirms the large errors for values of K_3, including K_3 equal zero (exclusion of the term), beyond the range indicated herein.

The column entitled "Balancing errors" indicates the differences between (a) the height fields obtained after balancing to the stream function and inverting again to height, and (b) the initial height field.

Table 4.2 lists the results of adjusting the value of K_2. Since K_3 was first adjusted, optimum values of this factor were used in adjusting K_2.

It will be noted from table 4.1 that a considerable portion of the

forecast errors is apparently due to the stream-function conversion. On 13 January, the conversion error amounts to 41% of the total forecast error, while on other days the ratios of errors range from 17% to 25%.

The trends of errors for varying K_3 all indicate a minimum error in the range -0.5 to -1.75 and also indicate the advantage of including 'Arnason's divergence term. From extrapolation of the curves in fig. 4.1, errors for K_3 equal zero are estimated to average about 20 feet above the least average for 24-hour forecasts.

The use of the factor K_2 does not seem to justify any deviation from unity, with improvements ranging from zero to only three feet for 24-hour forecasts.

Date	Balancing Errors	K_3						
		+1.25	-0.5	-0.75	-1.0	-1.25	-1.5	-1.75
14 Dec 1961	+ 9 59		+28 292 +25 452	(287) (436)	+29 28? +23 422	+29 280 +23 412	+29 280 +23 405	+29 282 +23 403
15 Dec 1961	+14 52		+21 284 - 2 405	(275) (386)	+20 268 - 2 371	+20 263 - 1 360	+20 261 - 1 353	+20 260 - 1 351
13 Jan 1962	+39 91		+50 221 +44 337	+50 222 +43 335	+50 225 +42 338	(230) (346)	+49 238 +41 358	(251) (377)
17 Jan 1962	+26 63	+14 316 +58 494	(258) (386)	+13 255 +59 385	+13 255 +60 ?86	+13 258 +60 391	(265) (404)	(276) (428)
21 Jan 1962	+12 50		(256) (393)	+10 250 +24 391	+10 248 +24 391	+10 249 +24 394	+10 251 +24 402	(256) (419)
Averages	63		262.2 394.6	257.8 386.6	255.8 381.6	256.0 378.6	259.0 384.4	265.0 395.6

Results of adjusting K_3

Table 4.1

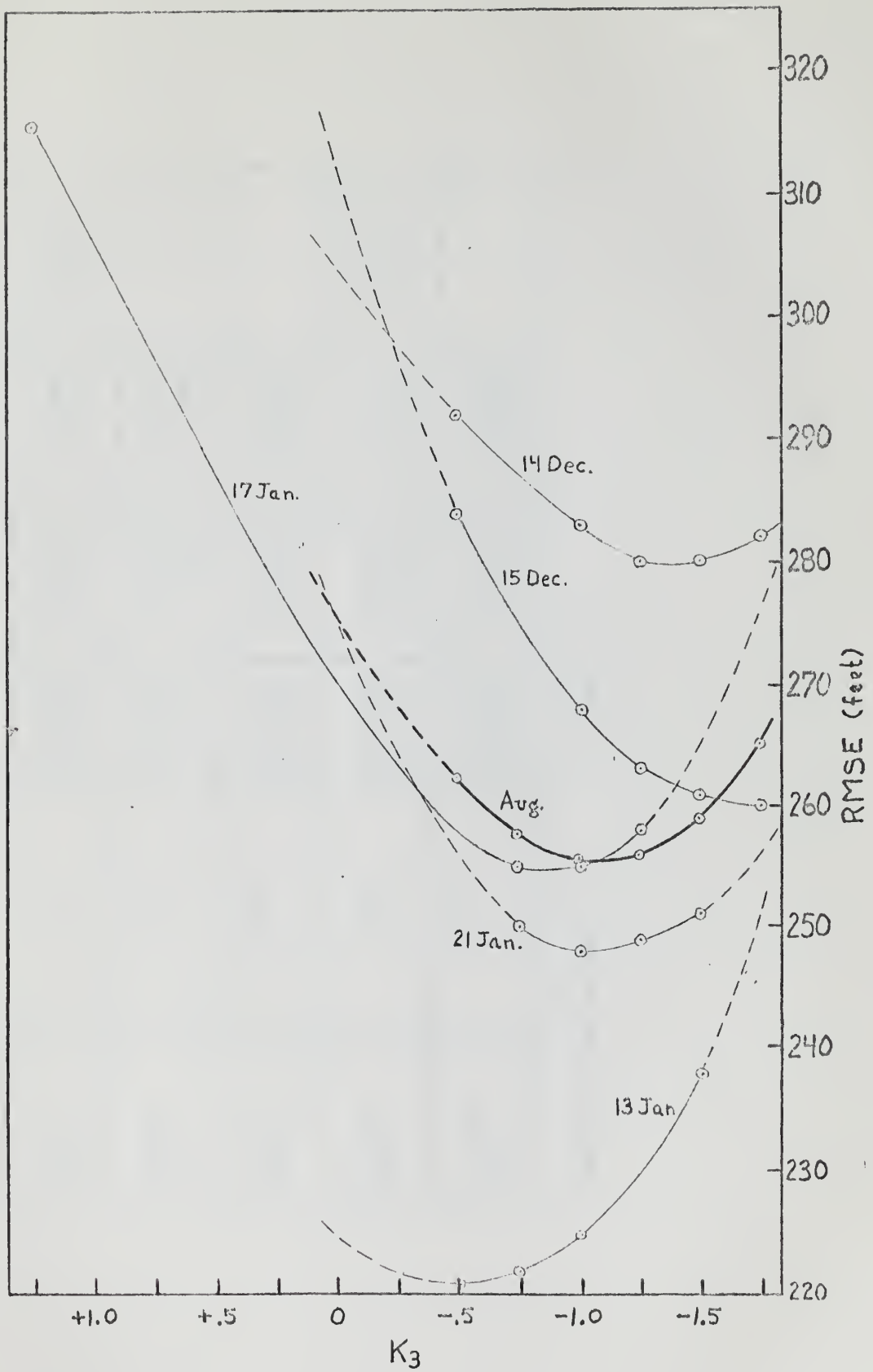

Fig. 4.1-Trends of RMSE values, 24-hour forecasts.

Date	K_3	K_2			
		1.0	0.9	0.8	0.7
14 Dec 1961	-1.5	+29 280 +23 405	+29 277 +27 389	+30 280 +31 383	+30 287 +34 388
15 Dec 1961	-1.75	+20 260 - 1 351	+21 259 0 349	+22 266 + 1 358	
13 Jan 1962	-0.5	+50 221 +44 337	+51 221 +45 331	+51 228 +46 335	
17 Jan 1962	-1.0	+13 255 +60 386	+13 255 +61 384	+13 261 +61 388	(K_2 = 0.75) +13 267 +61 394
21 Jan 1962	-1.0	+10 248 +24 391	+10 246 +24 390	+11 252 +23 403	

Results of adjusting K_2 Table 4.2

Figs. 4.2 through 4.4 depict the 13 January analyzed height field, the 14 January analyzed height field, and the 13 January, 24-hour forecast height field verifying on 14 January, respectively. In fig. 4.4 the initial (13 January) and observed (14 January) characteristics of certain of the systems are superimposed upon the forecast (for 14 January) field to indicate contrasting features. Initial features are dotted, and observed are dashed.

The following characteristics may be noted:

(1) In the western Pacific, the forecast of the short-wave trough was very much in agreement with its actual movement and intensity. No cyclogenesis occurred in this system and forecast errors were near zero in the area of the trough.

(2) The eastern Pacific low occurring on 13 January almost completely dissipated in 24 hours. The forecast position of this low is nearly that of the 14 January trough identifying the system. Height errors in excess of 700 feet are due to cyclolysis, which of course is not provided for in the model.

(3) In the Alaskan ridge, cyclogenesis occurred from 13 to 14 January in the NW portion, accounting for errors up to 600 feet. The ridge, however, was well forecast.

(4) The trough off the Atlantic coast of the U. S. was forecast to move in agreement with observation, but cyclogenesis again resulted in errors of about 400 feet.

(5) The low initially over the central Mediterranean moved into a cut-off position south of a blocking high. The forecast movement was in fair agreement, although a bit short, but accompanying cyclogenesis raised errors to about 600 feet. The forecast position of the blocking high was

good, but again, anticyclogenesis in the high and the ridge to the northeast introduced forecast errors of 400 feet and 600 feet, respectively.

Elsewhere on the map, the significant errors seem generally to be due to development processes and not to movements of the systems. These observations were corroborated by investigation of another sequence of maps produced in the investigation.

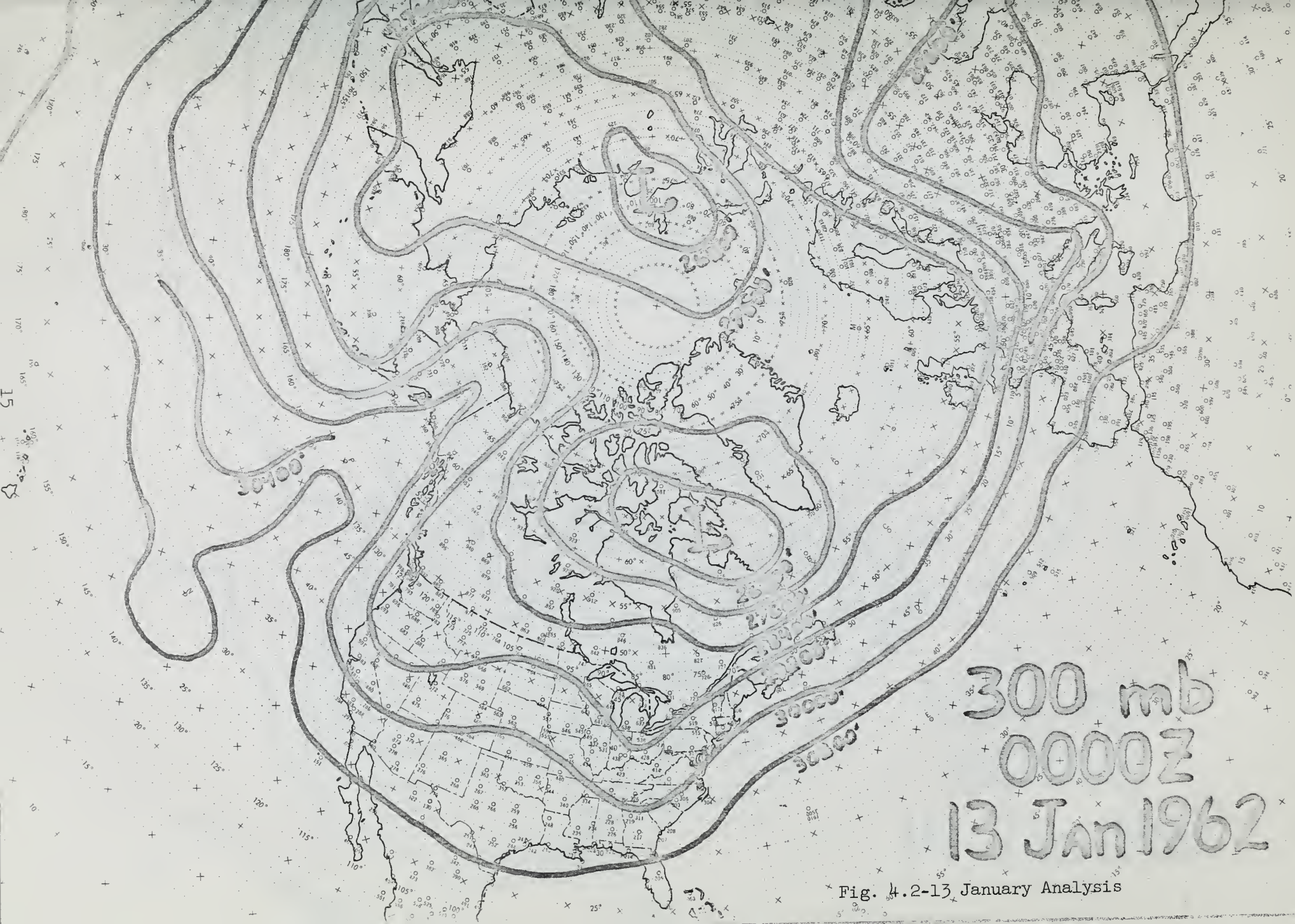

Fig. 4.2-13 January Analysis

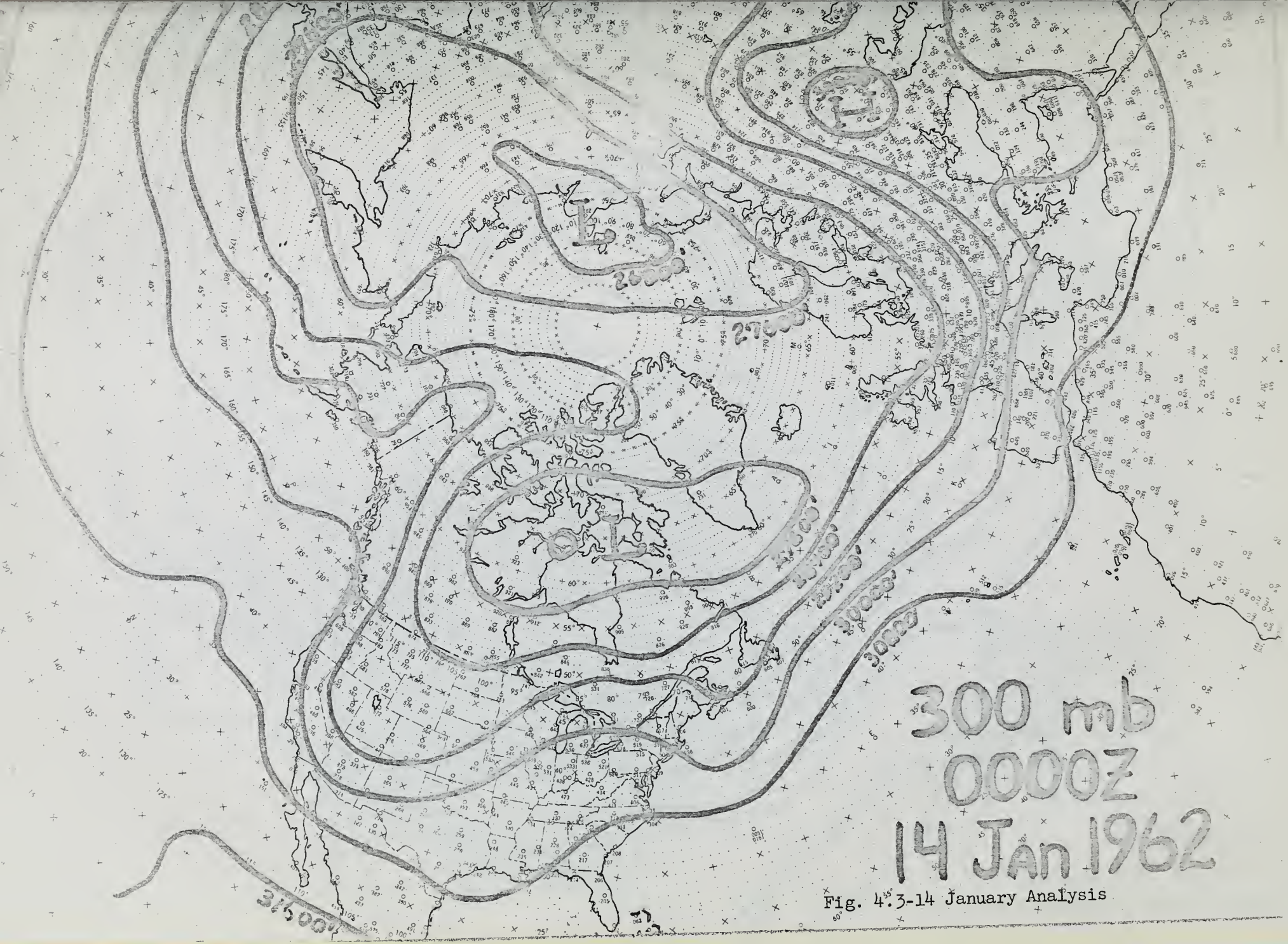

Fig. 4.3-14 January Analysis

Fig. 4.4-13 January, 24-hour Forecas

5. Conclusions.

It is noted from the averaged errors in table 4.1 that there are only limited differences in results over the range of K_3 values indicated. It was apparent, however, that sizable differences occur as K_3 is extended beyond this range, and of particular interest is the advantage over exclusion of the term (K_3 equals zero). These results indicate an optimum value for K_3 of about -1.0.

Even though varying K_2 did not yield significant differences in this investigation, it is possible that a greater number of cases might do so, particularly if some other season is considered. Only data from December, 1961 and January, 1962 were used.

Taking note of the large errors encountered in converting to a stream function, it is possible that a geostrophic model, not requiring such conversions, might reduce total errors somewhat. It is hoped that this investigation can be accomplished in the near future.

The model developed in this paper seems to fulfill its intended purpose, that is, forecasting realistic displacements unaffected by uncontrolled developments. With an understanding of its limitations, a forecaster should have here a useful tool, when supplemented by techniques for development prediction, to forecast pressure systems at the 300-mb level more easily and accurately.

BIBLIOGRAPHY

1. 'Arnason, G., A study of the dynamics of a stratified fluid in relation to atmospheric motions and physical weather prediction, Tellus, 13 (2), pp 156-170, May, 1961.

2. Charney, J. G., On a physical basis for numerical prediction of large-scale motions in the atmosphere, J. of Meteor., 6 (6), pp 371-385, Dec. 1949.

3. Cressman, G. P., Barotropic divergence and very long atmospheric waves, Monthly Weather review, 86 (8), pp 293-297, Aug. 1958.